tained to gain additional information concerning the excited states of these CT complexes. Contour plots of the charge density differences are shown in Figure 3. It can be seen that the first-excited-state transition corresponds to a $n \rightarrow \pi^*$ transition. Thus, there is a progressive increase in the $n \rightarrow \pi^*$ energy gap in going from $NH_3 \cdot SO_2$ to $TMA \cdot SO_2$. For $NH_3 \cdot SO_2$ the second, third, and fourth excited states also correspond to $n \rightarrow \pi^*$ transitions. However, the fifth state strongly resembles a diffuse s orbital (Figure 3).

Vibrational Frequencies and Infrared Spectra

To facilitate future characterization of the 1:1 and 2:1 amine·SO_2 CT complexes in the gas phase, we have reported the complete set of calculated (unscaled) harmonic frequencies (Tables IX) and their computed infrared spectra (Figure 4). First, we note that the bending mode of SO_2 is the dominant band in all spectra. The calculated frequency changes of the antisymmetric (ν_1) and symmetric (ν_2) stretching and bending (ν_3) vibrations of the SO_2 subunit are presented in Table X. Vibrational frequencies of SO_2 calculated at the HF/6-31G(d) level are found to be an average ~15% greater than the experimental frequencies,[31] and therefore the fundamental frequencies of the SO_2 subunit calculated here are scaled by 0.87 for comparison with experiment. As can be seen in Table X, the calculated ν_1 shifts are at higher wavenumbers relative to the monomer SO_2, whereas both ν_2 and ν_3 shifts are at lower wavenumbers. These results are in good accord with the experimental data.[5] The frequency shifts for ν_1 are relatively constant. On the other hand, there is a progressive increase in the magnitude of ν_2 and ν_3 shifts in both the 1:1 and 2:1 series, with larger shifts predicted for the 2:1 series. The trend of the frequency shifts correlates well with the strength of the donor-acceptor interaction. The calculated ν_2 and ν_3 shifts are smaller than the experimental values. These differences are attributed to the deficiencies of the HF/6-31G(d) geometries. Frequencies calculated at the MP2/6-31G(d) level should provide better comparisons with experiment.

(31) Shelton, R. D.; Nielson, A. H.; Fletcher, W. H. *J. Chem. Phys.* **1953**, *21*, 2178.

Conclusions

Several interesting points have been revealed by this study: (1) Inclusion of electron correlation is essential for the proper description of the N-S donor-acceptor bond in the amine·SO_2 complexes, especially for the larger complexes such as $TMA \cdot SO_2$. The calculated N-S bond lengths of $NH_3 \cdot SO_2$, $MA \cdot SO_2$, $DMA \cdot SO_2$, and $TMA \cdot SO_2$ at the MP2/6-31G(d) level are 2.80, 2.62, 2.46, and 2.36 Å, respectively. The calculated geometry of $TMA \cdot SO_2$ is in close agreement with the microwave data. (2) The enthalpies of formation (ΔH, 298 K) of $NH_3 \cdot SO_2$, $MA \cdot SO_2$, $DMA \cdot SO_2$, and $TMA \cdot SO_2$, computed using the MP3/6-31+G-(2d,p)//MP2/6-31(d) procedure, are 4.5, 6.7, 7.9, and 10.7 kcal mol^{-1}, respectively. The calculated ΔH value of $TMA \cdot SO_2$ agrees well with the experimental value of 9.7 kcal mol^{-1}. The trends of binding energy and N-S bond length are in good accord with the chemical intuition that a methyl group is a stronger electron donor than hydrogen. (3) All the 2:1 CT complexes are predicted to be thermodynamically stable with respect to dissociation into the 1:1 complex and amine, with binding energies smaller than the corresponding 1:1 complexes. As $(NH_3)_2 \cdot SO_2$ has been observed experimentally, the larger 2:1 complexes ($MA_2 \cdot SO_2$, $DMA_2 \cdot SO_2$, and $TMA_2 \cdot SO_2$), with greater calculated formation enthalpies, should be experimentally accessible species. (4) The N-S bonds of the amine·SO_2 CT complexes exhibit characteristics of a weak closed-shell interaction, with strong electrostatic forces. The calculated amount of charge transfer correlates well with the stabilities of the amine·SO_2 donor-acceptor complexes. (5) The calculated charge-transfer band, corresponding to a transition of $TMA \cdot SO_2$ (at CIS/6-311+G(d,p) level), is 258 nm, in good accord with the experimental value of 276 nm. The corresponding CT bands for $NH_3 \cdot SO_2$, $DMA \cdot SO_2$, and $DMA \cdot SO_2$ are predicted to be 283, 274, and 268 nm, respectively. (6) Significant frequency shifts are calculated for the fundamental vibrations of SO_2 subunit as a result of complex formation. The calculated frequency shifts for the 1:1 CT complexes are consistent with the experimental data.

Acknowledgment. This research was supported by a grant from the National Institutes of Health.

Solvent Effects on the Barrier to Isomerization for a Tertiary Amide from ab Initio and Monte Carlo Calculations

Erin M. Duffy, Daniel L. Severance, and William L. Jorgensen*

Contribution from the Department of Chemistry, Yale University, New Haven, Connecticut 06511-8118. *Received March 11, 1992*

Abstract: The effects of solvation on the free energies of activation for rotation about the carbonyl C-N bond in *N*,*N*-dimethylacetamide (DMA) have been examined through a combination of gas-phase ab initio calculations and solution-phase statistical mechanics simulations. The geometries of the planar ground state and the transition states with the nitrogen lone-pair anti and syn to the oxygen were optimized with the 6-31G(d) basis set. Subsequent calculations of the vibrational frequencies and correlation energies (MP4(fc)SDTQ/6-31G(d)//6-31G(d)) predict $\Delta G^{\ddagger}$'s of 14.6 and 18.7 kcal/mol for the anti and syn transition states at 298 K. NMR measurements have yielded a gas-phase $\Delta G^{\ddagger}$ of 15-16 kcal/mol. Solute-solvent potential functions were refined by fitting to results of 6-31G(d) calculations for the ground and transition states interacting with a water molecule in 17 low-energy orientations. These potentials were used in Monte Carlo simulations that yielded the changes in free energies in solvation in TIP4P water and the OPLS model of carbon tetrachloride. The observed ca. 2-kcal/mol increase in $\Delta G^{\ddagger}$ for water versus the aprotic solvent was reproduced; however, only a 0.4-kcal/mol barrier increase was computed for CCl_4 relative to the gas phase, while the experimental shift is 1-2 kcal/mol. The discrepancy may come from amide aggregation and variations in the transmission coefficient, whereas an explanation involving activation volumes is rejected. It is also predicted that the syn transition state becomes competitive with the anti in water, and hydrogen bonding analyses clarify the origin of the differential hydration.

Introduction

The importance of cis/trans isomerization about peptide bonds is emphasized by the role of proline isomerization in protein folding and by the recent findings that the binding proteins (immunophilins) for the immunosuppressive agents cyclosporin A, FK506, and rapamycin are peptidyl-prolyl cis/trans isomerases (rota-

0002-7863/92/1514-7535$03.00/0

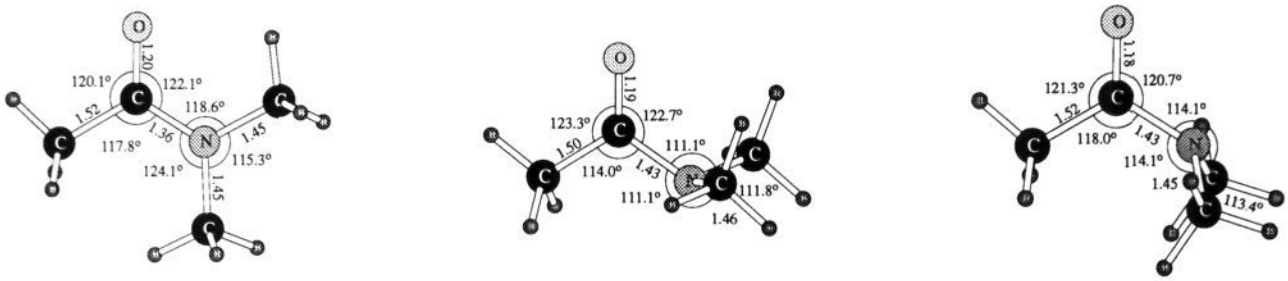

Figure 1. Structures of the DMA ground state and anti and syn transition states optimized with the 6-31G(d) calculations. Selected distances in angstroms and angles in degrees are given. Full details are available upon request.

masses).[1,2] Even with the availability of the crystal structure for the complexes of FK506 and rapamycin with their immunophilin, FKBP-12,[3] the mechanism of rotamase action is unclear. However, it is striking that the binding site in FKBP-12 is rich with hydrophobic residues, particularly Phe, Trp, and Tyr, such that it approximates an environment akin to a liquid aromatic hydrocarbon. This suggests the possibility of a relatively nonspecific mode of catalysis because it is known that the isomerization of amides is retarded in progressively more polar solvents.[4] The effects are large enough to account for the extent of catalysis that has been observed so far for peptide substrates of FKBP-12 and the immunophilin for cyclosprin A, cyclophilin.[5]

NMR measurements have been particularly valuable in quantifying such solvent effects for the isomerization of simple tertiary amides, and the original work on solutions[4,6] has more recently been extended to the gas phase.[7,8] The findings have been striking with medium-dependent variations as great as 4 kcal/mol for the free energy of activation. In the present paper, the problem is addressed through a combined quantum and statistical mechanical approach for the prototypical case of *N*,*N*-dimethylacetamide (DMA). Ab initio molecular orbital calculations are used to obtain the structures and gas-phase thermodynamic results for the ground state and two transition states. Additional ab initio calculations on complexes of these structures with a water molecule help in developing solute–solvent intermolecular potential functions. The potential functions are then used in Monte Carlo simulations for the isomerization of DMA in both carbon tetrachloride and aqueous solutioin. The calculations yield the solvent effects on the free energies of activation, $\Delta G^{\ddagger}$, for the isomerization and also illuminate the origin of the effects through detailed structural results including the analysis of the changes in hydrogen bonding.

Ab Initio Results for DMA

The requisite geometries for the ground state (GS) and the transition states with the nitrogen lone pair anti and syn to the oxygen were optimized via ab initio calculations with the 6-31G(d) basis set (Figure 1).[9] This split valence basis set with d-type polarization functions on non-hydrogen atoms has been shown to provide excellent results for the structures of neutral molecules.[10] This is supported by comparisons of the present predictions for the ground state (Figure 1) with results of electron diffraction measurements for *N*,*N*-dimethylformamide and *N*-methylacetamide, since gas-phase data do not appear to be available for DMA: r(CO) = 1.20 Å, r(CC) = 1.52 Å, r(CN) = 1.34 Å, r(N–CH_3) = 1.45 Å, ∠CCO = 124°, ∠OCN = 122°, and ∠CNCH_3 = 120°.[11] The structures for the ground and transition states in Figure 1 were fully optimized in C_1 and C_s symmetry, respectively. The heavy-atom framework for the ground state is essentially planar; constraining the geometry to C_s symmetry only raised the electronic energy by 0.07 kcal/mol at the 6-31G(d) level. Upon rotation to the transition states, the most significant structural changes are that the nitrogen is pyramidalized and the C–N bond lengthens from 1.36 to 1.43 Å. The modest contraction of the C=O bond by 0.01–0.02 Å has been noted previously for the isomerization of primary amides and was accompanied by an analysis that questioned the importance of amide resonance in the ground state.[12]

Table I. Thermodynamic Results for Isomerization of DMA in the Gas Phase[a]

ground state →	syn TS	anti TS	exptl[b]
ΔE_e^0	18.55	14.32	
ΔE_v^0	−0.53	−0.41	
$\Delta\Delta E_v^{298}$	−0.29	−0.31	
ΔH^{298}	17.73	13.60	15.8 ± 1.1
ΔS^{298}	−3.30	−3.39	1.5 ± 1.8
ΔG^{298}	18.71	14.61	15.3 ± 0.1

[a] Units are kcal/mol except cal/mol·K for ΔS. ΔE_e^0 is computed at the MP4(fc)SDTQ/6-31G(d) level, and the vibrational frequencies are from 6-31G(d)//6-31G(d) calculations. [b] Reference 8b.

Calculation of the 6-31G(d) vibrational frequencies confirmed the assignment of the anti and syn forms as transition states and allowed computation of the enthalpy, entropy, and free energy changes at 298 K. The electronic energy change was computed with inclusion of the correlation energy from a single point calculation at the MP4SDTQ/6-31G(d) level with frozen core orbitals (1s on C, N, and O).[10] The results are summarized in Table I. The anti TS has an electronic energy 14.3 kcal/mol above the ground state and 4.2 kcal/mol below the syn TS. These results are not very sensitive to the correlation treatment; the differences between the anti TS and ground state are 13.4 (HF/6-31G(d)), 14.8 (MP2), 13.6 (MP3), 13.5 (MP4D), 13.3 (MP4DQ), 13.7 (MP4SDQ), and 14.3 kcal/mol (MP4SDTQ), and the corresponding numbers for the syn versus the anti TS are 4.4, 4.3, 4.1, 4.1, 4.2, 4.2, and 4.2 kcal/mol. Based on previous results for primary amides, it is unlikely that extension of the basis set would shift these results by more than ca. 1 kcal/mol.[12]

(1) Fischer, G.; Schmid, F. X. *Biochemistry* **1990**, *29*, 2205.
(2) Schreiber, S. L. *Science* **1991**, *251*, 283.
(3) Van Duyne, G. D.; Standaert, R. F.; Karplus, P. A.; Schreiber, S. L.; Clardy, J. *Science* **1991**, *252*, 839. Van Duyne, G. D.; Standaert, R. F.; Schreiber, S. L.; Clardy, J. C. *J. Am. Chem. Soc.* **1991**, *113*, 7433.
(4) Drakenberg, T.; Dahlqvist, K.-I.; Forsen, S. *J. Phys. Chem.* **1972**, *76*, 2178.
(5) Albers, M. W.; Walsh, C. T.; Schreiber, S. L. *J. Org. Chem.* **1990**, *55*, 4984. Harrison, R. K.; Stein, R. L. *J. Am. Chem. Soc.* **1992**, *114*, 3464.
(6) Reeves, L. W.; Shaddick, R. C.; Shaw, K. N. *Can. J. Chem.* **1971**, *49*, 3683.
(7) Feigel, M. *J. Chem. Soc., Chem. Commun.* **1980**, 456. Feigel, M. *J. Phys. Chem.* **1983**, *87*, 3054.
(8) (a) Ross, B. D.; True, N. S.; Decker, D. L. *J. Phys. Chem.* **1983**, *87*, 89. (b) Ross, B. D.; True, N. S.; Matson, G. B. *J. Phys. Chem.* **1984**, *88*, 2675.
(9) GAUSSIAN 90, Revision F: Frisch, M. J.; Head-Gordon, M.; Trucks, G. W.; Foresman, J. B.; Schlegel, H. B.; Raghavachari, K.; Robb, M.; Binkley, J. S.; Gonzalez, C.; Defrees, D.J.; Fox, D. J.; Whiteside, R. A.; Seeger, R.; Melius, C. F.; Baker, J.; Martin, R. L.; Kahn, L. R.; Stewart, J. J. P.; Topiol, S.; Pople, J. A. Gaussian, Inc.: Pittsburgh, PA, 1990.
(10) Hehre, W. J.; Radom, L.; Schleyer, P. v. R.; Pople, J. A. *Ab Initio Molecular Orbital Theory*; Wiley: New York, 1986.
(11) Vilkov, L. V.; Akishin, P. A.; Presnyakova, V. M. *Z. Strukt. Khim.* **1962**, *3*, 5. Kitano, M.; Fukuyama, T.; Kuchitsu, K. *Bull. Chem. Soc. Jpn.* **1973**, *46*, 384.
(12) Wiberg, K. B.; Laidig, K. E. *J. Am. Chem. Soc.* **1987**, *109*, 5935. Wiberg, K. B.; Breneman, C. M. *J. Am. Chem. Soc.* **1992**, *114*, 831. Wiberg, K. B.; Hadad, C. M.; Rablen, P. R.; Cioslowski, J. *J. Am. Chem. Soc.* **1992**, *114*, 0000.

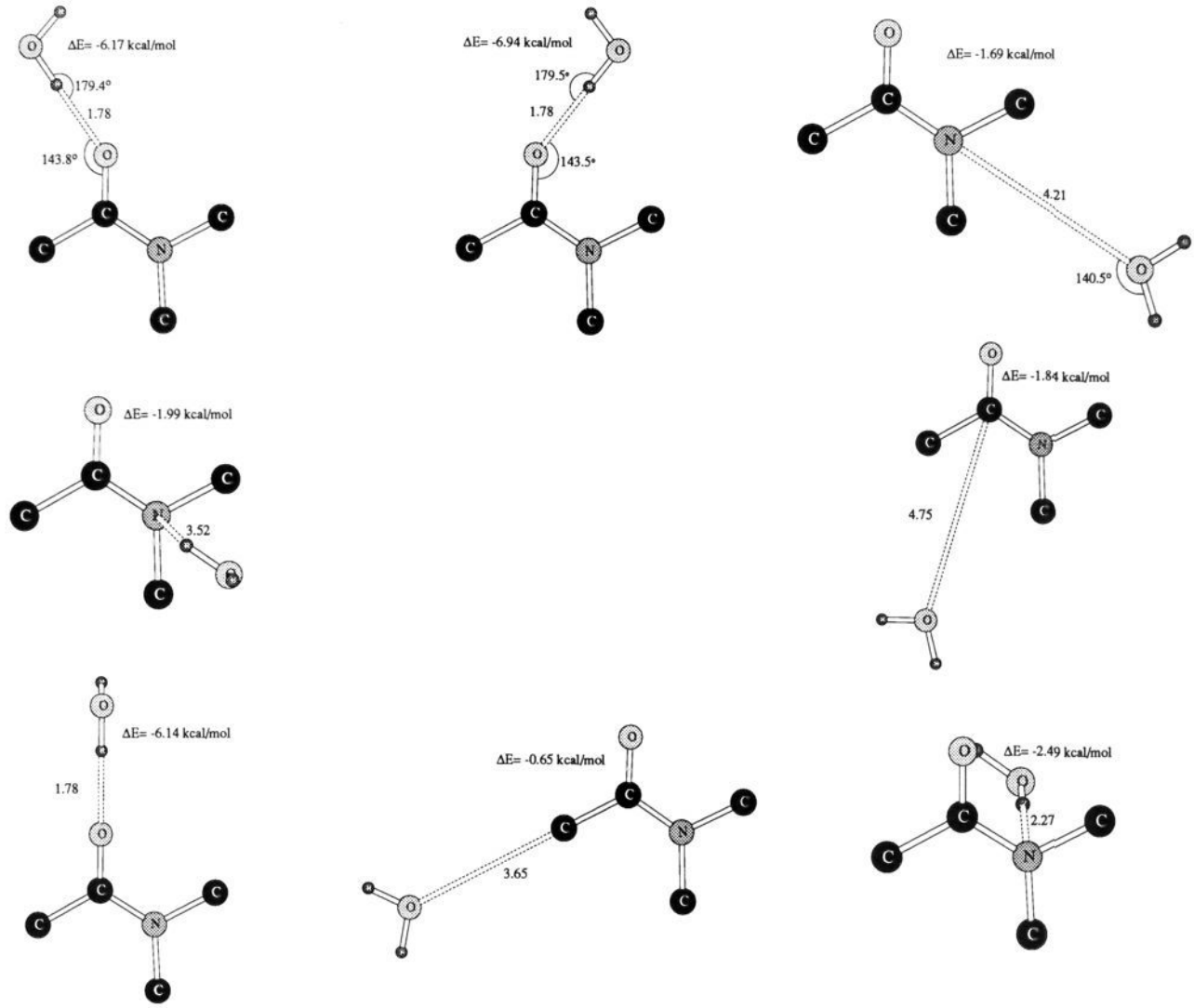

Figure 2. DMA–water complexes for the ground state. The structures are designated GS1 to GS8 from left to right starting at the top. The results of the partial optimizations with the potential functions are given.

In calculating the vibrational energies in Table I, the vibrational frequencies were scaled by 0.89.[10] In each case, the 7 (TS) or 8 (ground state) scaled frequencies below 500 cm^{-1} were treated as rotations ($E = RT/2$).[10] The imaginary frequency for the transition states is ignored in all thermodynamics calculations. In the present case, ΔH^{298} is then obtained from the sum of the changes in the electronic energy, ΔE_e^0, the zero-point vibrational energy, ΔE_v^0, and the thermal correction to the zero-point energy, $\Delta\Delta E_v^{298}$. The scaled frequencies were also used for the entropy calculation. In this case, the three lowest real frequencies, which correspond to rotations of the methyl groups, need to be treated as hindered rotations. Benson's prescription was followed with estimated barriers of 0 and 1.8 kcal/mol for the *N*-methyl rotations in the ground and transition states;[13] the barrier for the *C*-methyl rotation, ca. 1 kcal/mol, remains roughly the same during the isomerization and does not contribute to ΔS^{298}. The net contribution for the hindered rotations is then −1.6 cal/mol·K.[13] The resultant free energy of activation ($\Delta G^{\ddagger}$) for the anti TS, 14.6 kcal/mol, can be compared with the two gas-phase NMR results of 15.6 ± 0.1 and 15.3 ± 0.1 kcal/mol.[7,8b] The temperature dependence of the exchange broadening for the *N*-methyl protons was analyzed in the latter study and gave $\Delta H^{\ddagger}$ = 15.8 ± 1.1 kcal/mol and $\Delta S^{\ddagger}$ = 1.5 ± 1.8 cal/mol·K.[8b] The experimental uncertainties are greater here and the disagreements with the computed $\Delta H^{\ddagger}$ and $\Delta S^{\ddagger}$ are 2.2 kcal/mol and 4.9 cal/mol·K.

DMA–Water Complexes and Intermolecular Potential Functions

In order to calculate the solvent effects on $\Delta G^{\ddagger}$ from fluid simulations, it is necessary to have solute–solvent potential functions for the ground state and transition states. Though OPLS potential functions are available for the ground state of amides,[14] consistent parameters had to be developed for the transition states in the present study. This was accomplished with the aid of ab initio 6-31G(d) calculations for complexes of the ground state and two transition states interacting with a single water molecule. The 6-31G(d) basis set was chosen again in view of its previous success in describing hydrogen-bond strengths and geometries.[14,15] In all, 17 complexes were considered that emphasized low-energy hydrogen-bonded arrangements, as illustrated in Figure 2 for the ground state and in Figure 3 for the transition states. The 6-31G(d) optimizations were restricted to one distance and 0–2 bond angles in each case; the DMA geometries were fixed in their isolated 6-31G(d) forms (Figure 1) and the experimental geometry for an isolated water molecule was adopted (r(OH) = 0.9572 Å, ∠HOH = 104.52°), as in the TIP4P model of water.[16]

(13) Benson, S. W. *Thermochemical Kinetics*; Wiley: New York, 1968; p 45. See also: Truhlar, D. G. *J. Comput. Chem.* **1991**, *12*, 266.

(14) Jorgensen, W. L.; Swenson, C. J. *J. Am. Chem. Soc.* **1985**, *107*, 569. Jorgensen, W. L.; Swenson, C. J. *J. Am. Chem. Soc.* **1985**, *107*, 1489.

(15) Dill, J. D.; Allen, L. C.; Topp, W. C.; Pople, J. A. *J. Am. Chem. Soc.* **1975**, *97*, 7220.

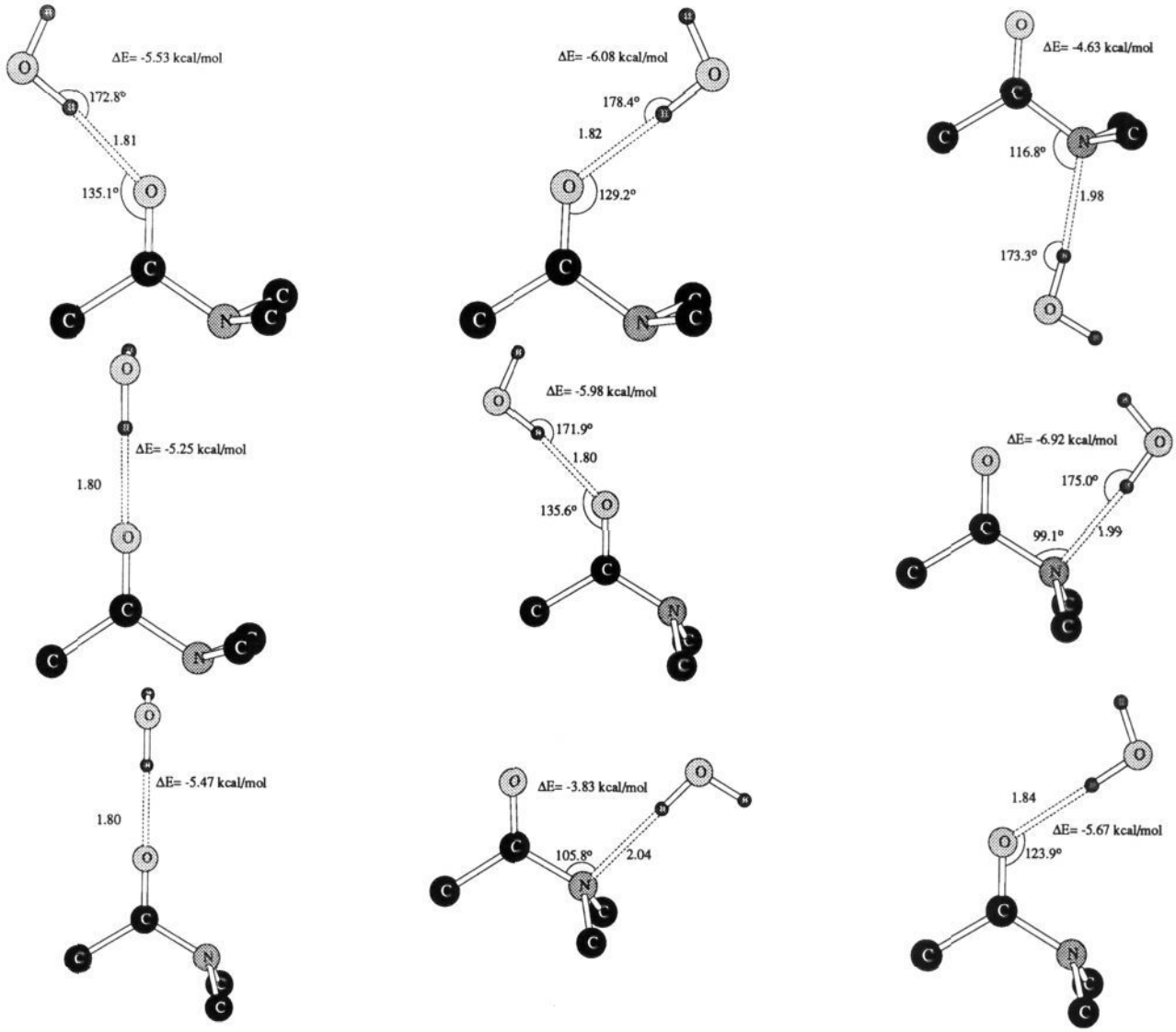

Figure 3. DMA–water complexes for the transition states. The structures are designated Anti1 to Anti4 and Syn1 to Syn5 from left to right starting at the top. The results of the partial optimizations with the potential functions are given.

Table II. Potential Function Parameters for DMA

atom	GS q, e[a]	GS q, e[b]	TS q, e[b]	σ, Å[a]	ϵ, kcal/mol[a]
CH_3(C)	0.000	0.020	0.160	3.910	0.160
C	0.500	0.530	0.467	3.750	0.105
O	−0.500	−0.480	−0.437	2.960	0.210
N	−0.570	−0.590	−0.590	3.250	0.170
CH_3(N)	0.285	0.260	0.200	3.800	0.170

[a] Original OPLS values from ref 14. [b] Charges from fitting to the 6-31G(d) results.

The OPLS united-atom model and Lennard-Jones parameters (σ, ϵ) for amides were adopted.[14] The potential energy between two molecules, ΔE_{ab}, consists of Coulomb and Lennard-Jones interactions between the interaction sites i on a and the sites j on b (eqs 1 and 2). The united-atom model for DMA has sites on

$$\Delta E_{ab} = \sum_i \sum_j \{q_i q_j e^2 / r_{ij} + 4\epsilon_{ij}[(\sigma_{ij}/r_{ij})^{12} - (\sigma_{ij}/r_{ij})^6]\} \quad (1)$$

$$\epsilon_{ij} = (\epsilon_i \epsilon_j)^{1/2}, \qquad \sigma_{ij} = (\sigma_i \sigma_j)^{1/2} \quad (2)$$

each atom except the methyl groups are treated as single sites centered on the carbons. Furthermore, the parameters for water have been taken from the TIP4P model.[16] Consequently, the only parameters that were varied to reproduce the ab initio complex energies and structures were the partial charges, q_i, for DMA. For a balanced fit to the 6-31G(d) data, minor variations to the OPLS charges[14] for the GS were made and one charge set sufficed for the TS's.

Table III. Computed Interaction Energies for DMA–Water Complexes[a]

complex[b]	6-31G(d) ΔE	eq 1 ΔE	complex[c]	6-31G(d) ΔE	eq 1 ΔE
GS1	−7.06	−6.17	Anti1	−5.58	−5.53
GS2	−6.39	−6.94	Anti2	−6.06	−6.08
GS3	−1.42	−1.69	Anti3	−4.93	−4.63
GS4	−1.95	−1.99	Anti4	−4.20	−5.25
GS5	−2.20	−1.84	Syn1	−5.84	−5.98
GS6	−5.61	−6.14	Syn2	−6.90	−6.92
GS7	−0.86	−0.65	Syn3	−4.28	−5.47
GS8	−1.39	−2.49	Syn4	−3.62	−3.83
			Syn5	−5.77	−5.67

[a] Interaction energies in kcal/mol. [b] Structures for the ground-state complexes from left to right in Figure 2. [c] Structures for the transition-state complexes from left to right in Figure 3.

The final parameters are listed in Table II, and the computed interaction energies from the 6-31G(d) calculations and from eq 1 for the 17 complexes are given in Table III. The complexes

(16) Jorgensen, W. L.; Chandrasekhar, J.; Madura, J. D.; Impey, R. W.; Klein, M. L. *J. Chem. Phys.* **1983**, *79*, 926.

are designated GS1 to GS8 going from left to right in Figure 2, and Anti1 to Anti4 and Syn1 to Syn5 going from left to right in Figure 3. The fitted charges give dipole moments of 3.72, 2.11, and 4.19 D for the planar, anti, and syn forms, while the 6-31G(d) values are 3.93, 2.12, and 3.75 D. Experimentally, the gas-phase dipole moment of DMA is 3.80 D.[17] Thus, the magnitudes of the dipole moments are reasonable, though the value from the partial charges for the syn TS is relatively too large. However, there is no exaggeration of the interaction energies for the syn form apparent in Table III, and it is convenient to have the single charge set for the transition states. Nevertheless, we did develop an alternative charge model for the syn form that gives virtually the same predictions (average $\Delta\Delta E$ = 0.08 kcal/mol) for the five syn complexes and has a dipole moment of 3.78 D. The charges on CH_3(C), C, O, N, and CH_3(N) are now 0.010, 0.710, −0.485, −0.695, and 0.230 e. Use of this model actually leads to a more negative free energy of hydration, as discussed below. The model is intended for this test purpose only, and not general use, because the magnitudes of the charges on C and N are inconsistent with normal OPLS values.[14]

The dipole moments are clearly sensitive to the choice of partial charges; as a further example, the original OPLS charges for the ground state yield a dipole moment of 4.34 D versus 3.72 D with the modified charges even though the largest individual charge change is only 0.03 e (Table II). The average error between the 6-31G(d) and fitted interaction energies for the 17 complexes is 0.4 kcal/mol. Use of the original charges for the ground state worsens the fit by making the attractions stronger by about 0.5 kcal/mol for GS1–GS6. This bias was avoided by using the new charges in the simulations, though the impact of the charge change on $\Delta\Delta G^{\ddagger}$ in water was also determined, as described below.

From the 6-31G(d) partial optimizations, the strength of the best hydrogen bond to the oxygen in the GS is −7.1 kcal/mol (GS1) versus −6.1 for the anti TS (Anti2), while the optimal interaction for the syn TS, −6.9 kcal/mol, has water hydrogens near both the nitrogen and oxygen (Syn2). Two difficulties arose in the fitting. It was not possible to reproduce the 6-31G(d) ordering for GS1 and GS2, so the compromise was to keep the magnitudes of the interaction energies similar with the ordering reversed. Thus, the ab initio calculations indicate a 0.7-kcal/mol preference for the complex with the water anti to the nitrogen, while the fitted potentials favor the water syn to the nitrogen by 0.8 kcal/mol. Many different charge distributions were tried with both united-atom and all-atom models without success in reproducing the ab initio order. It would be desirable to confirm the 6-31G(d) order with higher level optimizations including correlation corrections; the potential functions reflect some correlation effects through the Lennard-Jones terms. The only other notable discrepancy was for GS6, Anti4, and Syn3. These structures are similar with the C=O···H—OH fragment colinear. The interaction is uniformly too attractive with the potential functions, probably owing to the inadequacies of the simple point-charge description for the electron density on the oxygen.

The geometrical results from the potential functions compare well with the 6-31G(d) predictions. The average difference for the bond angles is 11° and the intermolecular distances are uniformly 0.1–0.2 Å shorter from the potential functions. The latter feature is normal and comes from the use of Lennard-Jones σ's that are appropriate for yielding correct liquid densities.[14]

Monte Carlo Simulations for the Free Energies of Solvation

Monte Carlo simulations were then carried out with these potential functions to compute the differences in free energies of solvation, ΔG_{sol}, in TIP4P water[16] and the OPLS model of carbon tetrachloride.[18] Free energy profiles were determined by incrementing the dihedral angle in 4.5° steps to convert the GS to the anti and syn forms. The BOSS program, Version 3.1,[19] was used and the free energy changes for each step were computed via statistical perturbation theory according to eq 3.[20] In the

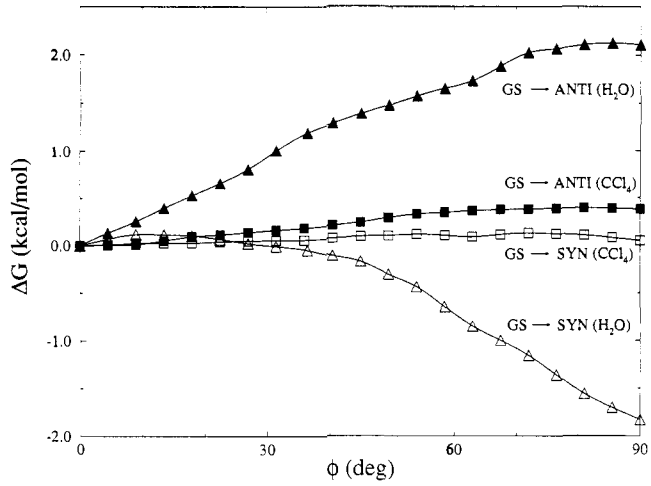

Figure 4. Computed changes in the free energies of solvation for converting the ground state to the anti and syn transition states in water and CCl_4 solution.

$$\Delta\Delta G_{sol} = G(\phi_j) - G(\phi_i) = -k_B T \ln \langle \exp(-(E(X,\phi_j) - E(X,\phi_i))/k_B T)\rangle_i \quad (3)$$

equation, $E(X,\phi_i)$ is the total energy of the system at dihedral angle ϕ_i, the average is taken from sampling at ϕ_i, and $E(X,\phi_j) - E(X,\phi_i)$ in the present case is equal to the difference in solute–solvent energies at the two values of the dihedral angle. No intramolecular energy terms have been included. The simulation is run with ϕ_i fixed, and the energy difference is evaluated for the perturbation to $\phi_j = \phi_i \pm 4.5°$. The procedures have been detailed previously in applications for the effects of hydration on the torsional profile of butane and the cis/trans equilibrium for *N*-methylacetamide.[21] It is noted that each simulation spanning 9° involved 1M (1×10^6) configurations of equilibration and 3M configuration of averaging in the NPT ensemble at 25 °C and 1 atm, the solute–solvent and solvent–solvent energy cutoffs were at 9.5 and 8.5 Å in water and at 12 and 12 Å in CCl_4, and 260 water or 127 CCl_4 molecules were included in periodic cubes with edge lengths of ca. 20 Å and 26 Å, respectively. The reported uncertainties are $\pm 1\sigma$ and were determined from fluctuations over separate averages of ca. 200K configurations. The uncertainties were kept low by the use of small perturbations ($\Delta\phi$ = 4.5°) and long runs.

The changes in ΔG_{sol} are shown in Figure 4. The shifts in water are pronounced with the anti TS being destabilized by 2.1 ± 0.1 kcal/mol and the syn TS being stabilized by 1.8 ± 0.1 kcal/mol relative to the ground state. This reduces the gas-phase free energy difference of 4.1 kcal/mol (Table I) between the syn and anti transition states to only 0.2 ± 0.1 kcal/mol. The anti form is still the favored transition state in water. However, it is less well-hydrated than planar DMA by 2.1 ± 0.1 kcal/mol, which is then the predicted increase in the free energy of activation for the isomerization in going from the gas phase to aqueous solution.

The trends in ΔG_{sol} follow the dipole moments in a nonlinear manner. As noted above, the present charge model makes the dipole moment for the syn form, 4.19 D, too large by ca. 0.4 D. The effect of using the alternative charge distribution with a dipole moment of 3.78 D was gauged by perturbing one charge distribution to the other over four simulations; switching to the model with the smaller dipole moment actually makes the free energy of hydration of the syn TS more negative by 0.63 ± 0.03 kcal/mol. Thus, in the present case, the magnitudes of the dipole moments

(17) Meighan, R. M.; Cole, R. H. *J. Phys. Chem.* **1964**, *68*, 503.
(18) Jorgensen, W. L.; Matsui, T. Unpublished. r(C–Cl) = 1.769 Å, σ_C = 3.80 Å, σ_{Cl} = 3.47 Å, ϵ_C = 0.050 kcal/mol, ϵ_{Cl} = 0.266 kcal/mol, and $q_C = -4q_{Cl}$ = 0.248 e. These give the correct density and ΔH_{vap} for CCl_4(l) at 25 °C and 1 atm.
(19) Jorgensen, W. L. BOSS, Version 3.1. Yale University: New Haven, CT, 1991.
(20) Zwanzig, R. W. *J. Chem. Phys.* **1954**, *22*, 1420.
(21) Jorgensen, W. L.; Buckner, J. K. *J. Phys. Chem.* **1987**, *91*, 6083. Jorgensen, W. L.; Gao, J. *J. Am. Chem. Soc.* **1988**, *110*, 4212.

are not as important as details of the description of the hydrogen-bonded complexes in controlling the free energy of hydration, or higher multipoles need to be included in the comparisons. Overall, the possible competitiveness of the syn TS in water has been raised.

The impact of perturbing the present charges for the ground state (3.72 D) to those for the original OPLS model (4.34 D) was also determined.[14] This change does lower ΔG_{sol} in TIP4P water by 1.56 ± 0.03 kcal/mol. Thus, if the original charges are used for the ground state, the anti TS would be destabilized by hydration by 3.7 ± 0.1 kcal/mol (1.56 + 2.1) and the syn TS would be stabilized by 0.2 ± 0.1 kcal/mol (1.56 − 1.8) relative to the ground state. The same charge change for the ground state was also studied in CCl_4 and was found to have no effect on ΔG_{sol} (−0.01 ± 0.01 kcal/mol).

By comparison, the solvent effects on the isomerization in CCl_4, which has an experimental dielectric constant of 2, are modest (Figure 4); the anti and syn TS's are destabilized by 0.38 ± 0.04 and 0.05 ± 0.04 kcal/mol with the new charges. Combination of the results for the anti form predicts an increase in $\Delta G^{\ddagger}$ upon transfer from CCl_4 to water of 1.7 ± 0.1 kcal/mol. Though this agrees well with the experimental shift of 2.0 kcal/mol,[4,6] the reported $\Delta\Delta G^{\ddagger}$ of 1.7–2.0 kcal/mol between the gas phase and CCl_4[6-8] is remarkably large and unreasonably greater than the present 0.38 kcal/mol. The prior rationale was that the activation volume, $\Delta V^{\ddagger}$, of +10 cm^3/mol for the DMA isomerization in organic solvents[22] and the internal solvent pressures of 1500–5000 atm provide increases via $P\Delta V^{\ddagger}$ of 1–2 kcal/mol in $\Delta G^{\ddagger}$.[8] This argument is flawed because $\Delta V^{\ddagger}$ comes from high-pressure NMR measurements of $(\delta\Delta G^{\ddagger}/\delta P)_T$, where P is the applied, external pressure;[22] the relation can then not be integrated using P as the internal solvent pressure. A positive or negative activation volume does not imply that a reaction is going to be retarded or accelerated by changing to solvents with a higher internal pressure at 1 atm external pressure. For example, Diels–Alder reactions have $\Delta V^{\ddagger}$'s of ca. −30 cm^3/mol; however, their rates at 1 atm vary little between the gas phase and a wide range of solvents except water.[23]

Some other issues may be considered that could compromise the ready comparisons of different isomerization rate data and the present results. Amide aggregation would be significant in the ca. 15 mol % CCl_4 solutions that have been studied.[6,8a] This effect has been noted previously[4,24] and raises the measured $\Delta G^{\ddagger}$ in less polar media to values closer to that for the neat amide, 18.2 kcal/mol in the case of DMA at 298 K.[4] Thus, the actual $\Delta G^{\ddagger}$ in CCl_4 is probably lower than the reported value, which would diminish the solvent effect relative to the gas phase. A second issue that may be particularly relevant, and difficult to handle, is the variation in the transition-state theory transmission coefficients (κ). The actual values of κ are unknown, so variations in κ are being absorbed into the reported free energies of activation. The more recent gas-phase study used $\kappa = 0.5$,[8b] while the solution studies and the present work have assumed $\kappa = 1$.[4] Just using the same κ in these cases would reduce the difference between the gas-phase and solution results by $RT \ln 2 = 0.4$ kcal/mol. However, barrier recrossings should increase, particularly for the modest-curvature ($\cos 2\phi$) potential, with increasing solvent cohesiveness.[25] Reduction of κ by a factor of 10 between the gas-phase and high-friction solvents would be in line with molecular dynamics results for alkane isomerizations[26] and would reduce the apparent range of $\Delta G^{\ddagger}$ by 1.4 kcal/mol. Trajectory calculations on the DMA isomerization in different media could give quantitative insights into this possibility.

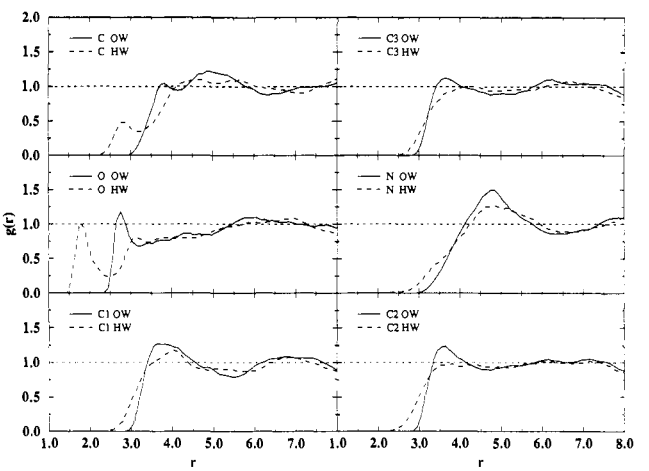

Figure 5. Computed DMA–water radial distribution functions for the ground state. C1 is the *C*-methyl group and C2 and C3 are the *N*-methyl groups syn and anti to the carbonyl oxygen; r in Å.

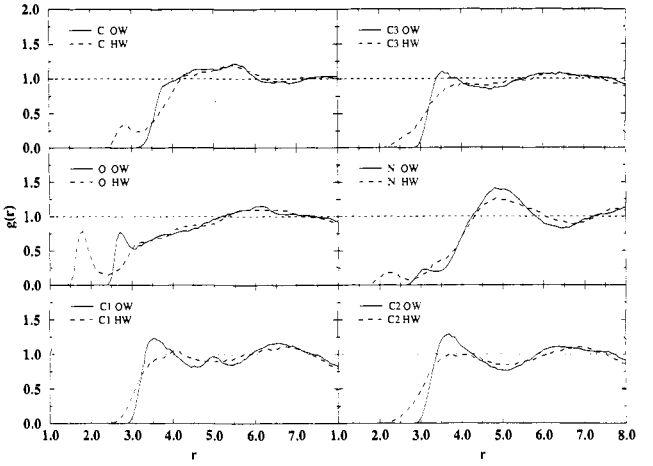

Figure 6. Computed DMA–water radial distribution functions for the anti transition state.

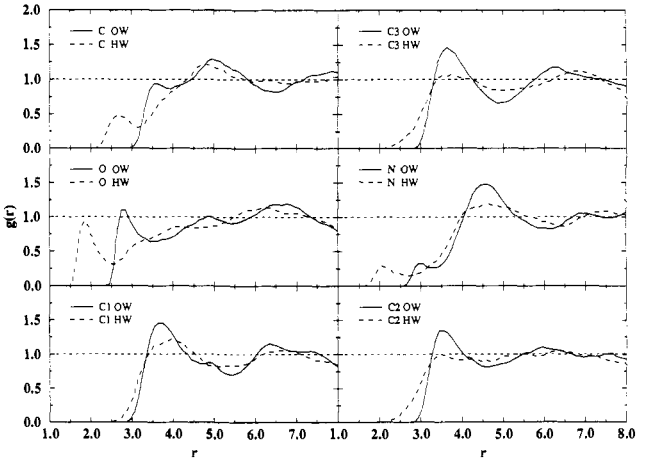

Figure 7. Computed DMA–water radial distribution functions for the syn transition state.

Solute–Solvent Structure and Hydrogen Bonding

In order to examine the origin of the differential hydration, various distribution functions were computed for the ground state and anti and syn transition states in separate simulations that

(22) Rauchschwalbe, R.; Volkel, G.; Lang, E.; Ludemann, H.-D. *J. Chem. Res. (M)* **1978**, 5323. Volkel, G.; Lang, E.; Ludemann, H.-D. *Ber. Bunsenges. Phys. Chem.* **1979**, *83*, 722.

(23) Sauer, J.; Sustmann, R. *Angew. Chem., Int. Ed. Engl.* **1980**, *19*, 779. Breslow, R.; Guo, T. *J. Am. Chem. Soc.* **1988**, *110*, 5613.

(24) Rabinovitz, M.; Pines, A. *J. Am. Chem. Soc.* **1969**, *91*, 1585.

(25) Truhlar, D. G.; Hase, W. L.; Hynes, J. T. *J. Phys. Chem.* **1983**, *87*, 2664. Hynes, J. T. *Annu. Rev. Phys. Chem.* **1985**, *36*, 573.

(26) Levy, R. M.; Karplus, M. A.; McCammon, J. A. *Chem. Phys. Lett.* **1979**, *65*, 4. Rosenberg, R. O.; Berne, B. J.; Chandler, D. *Chem. Phys. Lett.* **1980**, *75*, 162. Montgomery, J. A., Jr.; Holmgren, S. L.; Chandler, D. *J. Chem. Phys.* **1980**, *73*, 3688.

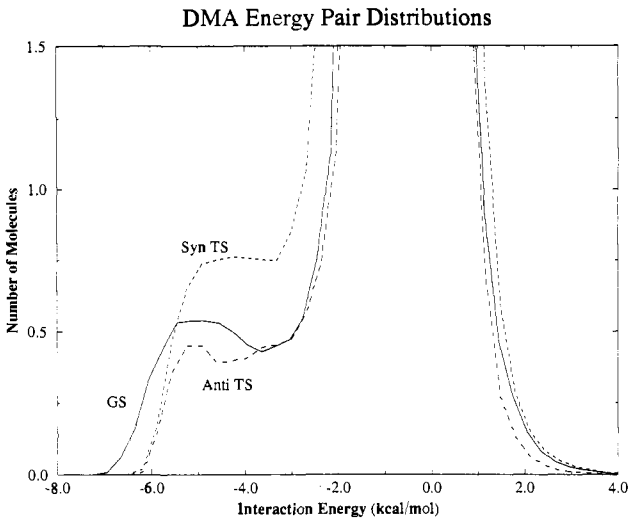

Figure 8. Computed DMA–water energy pair distribution functions. The units for the ordinate are number of water molecules per kcal/mol.

involved averaging over 4M configurations. A principal index of structure in liquids is radial distribution functions, $g_{xy}(r)$, which represent the probability of occurrence of an atom of type y at a distance r from an atom of type x, normalized for the bulk density of y atoms such that $g_{xy}(r) \rightarrow 1$ as $r \rightarrow \infty$. The computed radial distribution functions (rdfs) between DMA atoms and the H and O of water are shown in Figures 5–7. In these plots, C1 is the methyl carbon adjacent to the carbonyl oxygen, and C2 and C3 are the *N*-methyl carbons syn and anti to the carbonyl oxygen in the ground state that become equivalent in the transition states.

For the ground state (Figure 5), the most striking features are the first peaks in the O–O and O–H rdfs. These peaks reflect the water molecules hydrogen bonded to the carbonyl oxygen. Integration of the O–H first peak to the minimum at 2.5 Å reveals 1.7 hydrogens, which is the same as the number of oxygens in the first peak of the O–O rdf out to 3.1 Å. On the other hand, the N–H and N–O rdfs show no evidence of hydrogen bonding at the nitrogen; the N–H rdf out to 2.5 Å contains 0.01 hydrogen. The rdfs for the carbonyl C do show first peaks, shifted out by ca. 1 Å from the positions in the O–O and O–H rdfs, that can be assigned to the hydrogen bonded water molecules on the carbonyl oxygen. The rdfs involving the methyl group carbons are all relatively structureless and have the usual broad, weak first peaks at 3–4 Å for the first-shell water molecules about alkyl groups.[14]

Both sets of rdfs for the transition states (Figures 6 and 7) are similar to each other and show some clear differences from those for the ground state. Hydrogen bonding at the carbonyl oxygen is apparent in the first peaks of the O–H and O–O rdfs, but is diminished in magnitude for the anti TS (Figure 6). Integration of the O–H rdfs to 2.5 Å yields 1.1 and 1.9 hydrogens for the anti and syn forms. In addition, the N–H and N–O rdfs now have small first peaks that suggest in the rotated forms that there is some hydrogen bonding at nitrogen. The integrals of the N–H rdfs to 2.5 Å contain 0.4 and 0.6 hydrogen for the anti and syn transition states. The larger integrals for the N–H and O–H rdfs in the syn form need further analysis in terms of the actual numbers of hydrogen bonds that exist because water molecules that are hydrogen bonded to either site can possibly contribute to both rdfs.

Consequently, hydrogen bond analyses were performed for each form of DMA on 400 configurations that were saved every 10K configurations during the simulations. For this purpose, a hydrogen bond is required to feature a DMA–water interaction energy that is attractive by at least 2.25 kcal/mol and an N···HOH or O···HOH distance of no more than 2.5 Å. The geometrical cutoff is supported by the limits of the first peaks in the rdfs, while the energetic cutoff is an empirical one that has been used previously for pure water[16] and is supported by the characteristic shape of the solute–water energy pair distribution functions, as illustrated in Figure 8. These are plots of the number of water molecules that interact with the solute with the interaction energy given on the abscissa. The low-energy bands extend to about the −2.25-kcal/mol limit and contain the most bound water molecules. The spikes between −2 and +2 kcal/mol primarily reflect the many interactions with more remote water molecules in the bulk. The weaker low-energy band for the anti TS is consistent with its poorer hydration; however, the competition between the ground state and syn TS is unclear. The syn TS has the largest number of low-energy interactions, while the ground state has the most attractive individual interactions with water molecules.

Table IV. Results of Hydrogen Bond Analyses for DMA in Water[a]

	ground state	anti TS	syn TS
ave. no. H-bonds	1.55	1.31	1.81
ave. H-bond energy	−4.52	−4.05	−4.16
no. H-bonds on O	1.55	1.03	1.47
ave. energy	−4.52	−4.27	−4.21
no. H-bonds on N	0.00	0.29	0.35
ave. energy	0.00	−3.25	−3.95

[a] Results from the Monte Carlo simulations at 25 °C and 1 atm. A hydrogen bond is defined by an interaction energy ≤−2.25 kcal/mol and an N···H or O···H distance ≤2.5 Å.

With the given definition of a DMA–water hydrogen bond, the findings in Table IV emerged. On the basis of results for different subsets of configurations, the values in Table IV are accurate to two significant figures. The hydrogen bonds have also been assigned to either the oxygen or nitrogen of DMA based on which atom has the shortest distance to one of the water hydrogens. The basic trends from the rdfs are supported. There are 1.55 hydrogen bonds with an average strength of −4.52 kcal/mol on the carbonyl oxygen in the ground state, and no hydrogen bonds on the nitrogen. Consistent with the ab initio results for the complexes and Figure 8, the ground state forms the strongest hydrogen bonds on average. Rotation to the anti TS reduces both the total number of hydrogen bonds (1.31) and their strengths (−4.05 kcal/mol), though 0.29 hydrogen bond now occurs at the nitrogen; i.e., there is a water molecule hydrogen bonded to the nitrogen about one-third of the time. The reduction of hydrogen bonds at the oxygen reflects both the lower polarity for the anti TS and the greater shielding by the two *N*-methyl groups that stagger the oxygen in the TS rather than the one eclipsing *N*-methyl group in the ground state. The syn transition state enjoys the largest number of hydrogen bonds (1.81) with 1.47 on the oxygen and 0.35 on the nitrogen. There is relatively little shielding of the carbonyl oxygen by the *N*-methyl groups in this case.

An important observation comes from multiplying the average number of hydrogen bonds by the average strength. This yields the total contribution to the hydration energy from the hydrogen bonds and is −7.0, −5.3, and −7.5 kcal/mol for the ground state and anti and syn transition states. Thus, the 2.1-kcal/mol higher free energy of hydration for the anti TS than the ground state (Figure 4) can largely be attributed to the poorer hydrogen bonding for the anti TS. However, only 0.5 kcal/mol of the 1.8-kcal/mol lower free energy of hydration for the syn TS can be assigned to the hydrogen bonding difference. The remainder appears to come from the larger number of more remote, attractive interactions with water molecules that is reflected in the low-energy band between −5 and −3 kcal/mol in the energy-pair distribution (Figure 8).

Conclusion

In summary, the present combined quantum and statistical mechanical investigations of the isomerization of *N*,*N*-dimethylacetamide lead to the following principal results. At the MP4(fc)SDTQ/6-31G(d)//6-31G(d) level, the gas-phase $\Delta G^{\ddagger}$ at 298 K is computed to be 14.6 kcal/mol for the anti transition state and 18.7 kcal/mol for the syn transition state. From the Monte Carlo simulations, transfer to dilute aqueous solution is predicted to destabilize the anti transition state relative to the ground state by 2.1 kcal/mol and stabilize the syn transition state by 1.8 kcal/mol. This places the anti transition state only 0.2

kcal/mol below the syn alternative in water. The poorer hydration that accompanies rotation from the ground state to the anti transition state was found to result from diminished hydrogen bonding to the carbonyl oxygen that is not made up by introduction of limited hydrogen bonding at the pyramidalized nitrogen. The enhanced hydration of the syn transition state results in part from greater hydrogen bonding in the region of confluence of the figurative nitrogen and oxygen lone pairs, and from more constructive longer-range interactions with water molecules. The solvent effects in CCl_4 are much less with the anti and syn transition states destabilized by 0.38 and 0.05 kcal/mol relative to the ground state. Thus, with addition of the gas-phase free energy difference, the syn transition state is not competitive in CCl_4. The predicted, substantial increase in $\Delta G^{\ddagger}$ between dilute CCl_4 and aqueous solution, 1.7 kcal/mol, is consistent with experimental estimates; however, the present calculations find a 1-2-kcal/mol smaller difference between the gas phase and CCl_4 solution than has been reported experimentally. The potential functions developed here may also be useful in future calculations for the transmission coefficient and for modeling related isomerizations in real and artificial enzymes.

Acknowledgment. Gratitude is expressed to the National Science Foundation and National Institutes of Health for support of this research, and to Professor Donald G. Truhlar for helpful insights.

Molecular Recognition of Potassium Ion by the Naturally Occurring Antibiotic Ionophore Nonactin

Tami J. Marrone and Kenneth M. Merz, Jr.*

Contribution from the Department of Chemistry, The Pennsylvania State University, University Park, Pennsylvania 16802. *Received March 13, 1992*

Abstract: Potential of mean force (PMF), free energy perturbation (FEP), and molecular dynamics (MD) computer simulations have been used to investigate the molecular recognition of K^+ by the ionophore nonactin in methanol. First, parameter sets for K^+ and Na^+ in methanol were developed such that they were able to reasonably reproduce the free energy of solvation of these ions as well as coordination numbers. Next, we computed the free energy of binding difference for $K^+ \rightarrow Na^+$ in nonactin and obtained a value of 1.0 ± 0.8 kcal/mol which is in good agreement with the experimental value of 2.0 ± 0.7 kcal/mol. To obtain an estimate of the absolute free energy of binding, we used PMF calculations. This was done only for K^+, and we found that our calculated binding energy was in good agreement with the experimental one (-6.4 kcal/mol versus -5.5 ± 0.6 kcal/mol). Analysis of the structures obtained along the PMF pathway yielded interesting details about the complexation process in nonactin. A brief discussion of the function of nonactin is also presented.

Introduction

Understanding at the molecular level how one molecule recognizes another is of fundamental importance to chemistry and biochemistry.[1] Antibiotic ionophores, such as valinomycin and the macrotetralide nonactin, have been studied in detail in order to understand how these molecules selectively recognize ions.[2] These naturally occurring molecules selectively bind a specific metal ion, which can be considered as a charged spherical "substrate", and transport it across the cell membrane to release it on the other side.[2] Under certain circumstances, synthetic macrocycles are also capable of performing this function.[3] Generally, ionophores preferentially bind a specific metal ion, but the selectivity scale varies widely among the naturally occurring ionophores with valinomycin having one of the highest K^+/Na^+ selectivities and nonactin having a lower K^+/Na^+ selectivity.[2] For these molecules to accomplish their transport function they must have several characteristics. First they must be able to bind a metal ion selectively and tightly while at the same time be flexible enough to release the ion fairly rapidly. Furthermore, to be compatible with a biomembrane, the ionophore must have a hydrophobic exterior while having a hydrophilic interior capable of binding an ion. Nonactin meets these requirements by having a balled hydrophobic exterior in the complexed form and showing conformational flexibility.

The crystal structures of the uncomplexed form[4] and the potassium complexed form[5] of nonactin, which are given in Figures 1 and 2, respectively, demonstrate the conformational flexibility of the molecule. The uncomplexed form has roughly S_4 symmetry in the solid state, and from PMR studies it appears that this structure and others are present in solution.[1,6] The K^+, Na^+, Cs^+, and NH_4^+ complexed structures for nonactin have all been solved.[5] They all adopt a very similar conformation, which has the cation sitting at the center of a cube formed from four ether and four carbonyl oxygens for a coordination number of eight.[1] This arrangement is obtained by twisting the molecule into a conformation that has been described as a seam of a tennis ball.[1]

Figure 3 gives a schematic representation of nonactin. There are several important things to note: first, the molecule consists of a single "residue" that is repeated four times. However, two of these residues have configurations around the methyl groups of *SS* and two are *RS*. This leads to an alternating *RS*, *SS*, *RS*, and *SS* pattern which when folded together in the complex form places the *RS* and *SS* residue pairs opposite one another. This observation will be important when we consider reaction pathways for ion association.

(1) (a) Cram, D. J. *Science* **1988**, *240*, 760. (b) Rebek, J. R. *Science* **1987**, *235*, 1478. (c) Lehn, J.-M. *Angew. Chem., Int. Ed. Engl.* **1988**, *27*, 89.
(2) (a) Dobler, M. *Ionophores and Their Structures*; Wiley: New York, 1981. (b) Ovchinnikov, Y. A.; Yivanov, V.; Shkrob, A. M. *Membrane Active Complexones*; Elsevier: Amsterdam, 1974. (c) Eisenmann, G., Ed. *Membranes: A Series of Advances*; Marcel Dekker: New York, 1975; Vol. 3.
(3) (a) Kirch, M.; Lehn, J.-M. *Angew. Chem., Int. Ed. Engl.* **1975**, *14*, 555. (b) Deitrich, B. *J. Chem. Educ.* **1985**, *62*, 954.
(4) Dobler, M. *Helv. Chim. Acta* **1972**, *55*, 1371.
(5) (a) K^+ complex: Dobler, M.; Dunitz, J. D.; Kilburn, B. T. *Helv. Chim. Acta* **1969**, *52*, 2573. (b) Na^+ complex: Dobler, M.; Phizackerley, R. P. *Helv. Chim. Acta* **1974**, *57*, 664. (c) Cs^+ complex: Sakamati, T.; Iitaka, Y.; Nawata, Y. *Acta Crystallogr.* **1977**, *B33*, 52. (d) NH_4^+ complex: Neuport-Laves, K.; Dobler, M. *Helv. Chim. Acta* **1976**, *59*, 614.
(6) Prestegard, J. H.; Chan, S. L. *Biochemistry* **1969**, *8*, 3921.

0002-7863/92/1514-7542$03.00/0